Chapter 5

Air-Suspended Silicon Micro-Bridge Structures for Metal Oxide-Based Gas Sensing

Keshavaditya Golla and Eranna Golla

Additional information is available at the end of the chapter

http://dx.doi.org/10.5772/62647

Abstract

Maintaining specific temperature is a key parameter for most of the gas sensing materials, particularly for metal oxide-based thin film layers, to operate them more efficiently to detect different gaseous (or vapor) species at ppm and ppb concentration levels. For field applications, battery-operated micro-gas-sensors, power dissipation and the required temperature stability are to be maintained with a close tolerance for better signal stability and also to analyze the generated data from the sensing element. This chapter mainly focuses on several metal oxide films to highlight the base temperature and its creation on silicon-based platforms. Air-suspended structures are highlighted, and a comparison is drawn between simple and MEMS-based structures from the power dissipation point of view. Ease of fabrication and operation limitations are explained with fabrication issues.

Keywords: Metal oxide thin films, Gas sensing devices, Platinum micro-heater, Platinum resistance thermometer, MEMS, Surface micromachining

1. Introduction

A lot of research effort has been directed toward the development of miniaturized gas sensing devices, particularly for toxic gas (or vapor) detection and also for pollution monitoring in general and industrial ambience. Such devices should allow continuous monitoring of the concentration levels of particular gaseous species in a quantitative and selective way to enable one to take specific remedial action against the prevailing situations. Though various techniques are available for gas detection, studies based on gas chromatography methods are popular for their accuracy in quantifying the species. This is a major chemical analysis instrument for

separating species in a complex sample. The system uses a flow-through narrow tube, known as the column, through which different air samples pass in a gas stream at different rates. Depending on their various chemical and physical properties and their interaction with a specific column filling, they get separated and are subsequently detected. For field applications, such instrumentation usage has practical limitations, and hence, portable devices are preferred. In this respect, solid-state metal oxides offer a wide spectrum of materials, and their sensitivities for different gaseous species, thus making it a better choice for miniaturized sensing devices. However, the efforts have not yet reached commercial viability for many gaseous species because of problems associated with the sensor fabrication technologies applied to these micro-gas-sensing devices.

Primarily the gas detection method is based on the changes in the electrical properties of the sensing films, such as electrical resistance (or conductance); in this case, they are thin metal oxide films. The key detection process in these films is the change of the oxygen concentration surrounding the sensing element. This is caused by the adsorption of the test gaseous species and subsequent heterogeneous catalytic reaction of oxidizing and reducing gaseous species to which they are interacting at the surface. The electrical conductivity depends on the gas atmosphere and on the temperature of the sensing material exposed to the test gas. The signal generated from the sensing element strongly depends on the temperature of the element also. Hence, one has to keep the temperature of the element with an external heater such as platinum in most of the cases. Other elements include doped polycrystalline silicon and nichrome (alloy of nickel and chromium) for this application.

Almost all the solid materials interact with the surrounding areas with their exposed surfaces. The physical and chemical compositions of these solid surfaces determine the nature of these interactions. The surface chemistry will influence many properties, and a gas species interaction is one of the key parameter for gas sensing phenomena. In these reactions, only very small proportions of the atoms of most solids, that too very close to surface areas, participate and interact. These interactions also depend upon the shape and surface roughness conditions. With the increasing demand for better gas sensors, of higher interactions and greater selectivity, intense efforts are being made to find suitable solid materials with the required surface and bulk properties useful for these applications. Material properties and the gaseous species structure cum polarity of the gas molecule play a key role at this stage. It is always desired that the material to be used in the fabrication of these sensors do interact with the gaseous species and upon removal of the interacting species the material ability to return to its initial state, which has induced the change, of its electrical properties. Not many sensor materials show this surface property.

2. Metal oxide thin films for sensing applications

The gas sensors using metal oxide semiconductors have been the subjects of extensive investigations for more than four decades primarily focusing on the SnO_2 material. In more recent research efforts, the interest has shifted to some other promising metal oxide thin films,

http://dx.doi.org/10.5772/62647

with very interesting detection properties that they exhibit as promising gas sensing materials. Using new metal oxides has several technological advantages, such as: simplicity in element formation and definition of device structure, excellent chemical stability in harsh environment, relatively low material cost for their fabrication, robustness in practical field applications, and adaptability to wide variety of reductive or oxidative industrial ambient conditions. Fairly good studies have been carried out on these groups of gas sensing materials, and at present, it is an active field of research, and many research teams are actively involved for their development. Nano-structured metal oxide films are gaining popularity because of their surface features exhibited by providing additional surface area achievable in these features [1] for more gaseous interactions.

Metal oxide semiconductor gas sensors work mainly on the principle of reversible change of their electrical resistance when exposed to the gas under study. This property is exhibited by most of the sensing materials that are induced by the changes in their chemical environment. It is found that the adsorption of atomic and molecular species on the inorganic semiconductor surfaces affect the surface properties not only related to the electrical conductivity but also influence the material surface potential. Careful study of these variations in the ambient atmosphere and applying them for gas detection scheme will help to analyze the environment to which it is exposed. This change permits detection and nature of the gas and also on the magnitude of change in chemical environment. In almost all the cases, suitability of sensing material, to be used in the fabrication of chemical gas sensor, depends on its ability to return to its initial stage upon removal of cause that induced the change. Metal oxides are better choice in most of the cases to achieve this key point. However, this issue is one of the toughest problems to select the combination of sensing material and the gas/vapor to be detected. Many breakthroughs are expected in this field of research in near future.

As mentioned earlier, the gas (or vapor) detection technique is primarily based on the change in their electrical resistance of the metal oxide films [2] upon their exposure to the test gas under study. The principal detection process is the change of oxygen concentration at the surface of these sensing metal oxides, caused by the adsorption of the test gas and subsequent heterogeneous catalytic reactions of the gas under study. These test gases could be either oxidizing and/or reducing gaseous species. However, these reactions are temperature sensitive and the electrical conductivity (or variation) depends on the nature of the test gas and also on the temperature of the sensing material exposed to this gas. The signal, typically defined as the ratio of resistance variation, generated from the sensing element strongly depends on the operating temperature of the sensing element. It is necessary to keep the temperature of this sensing element, with an external heater, such as platinum, at a predetermined temperature and is generally attached to the sensing element or should be a part along with it. The heating element should be capable of producing higher temperatures than the typical operating temperature ranges of the sensing element during the operation. This excess temperature is necessary and is purpose built and will help for the periodical regeneration of the sensor surface to drive away the unwanted surface adsorbents. The regeneration process is normally carried out at a temperature above the highest temperature at which the sensing devices are

typically operated for maximum sensitivity. Typical values are about 50°C in most of the cases. This will drive out other unwanted gaseous species attached to the surface.

3. Importance of sensor temperature

Operating temperature of gas sensors, based on metal oxides, is a key issue and most important parameters for the operation of any sensor. Different oxide materials respond differently to various gaseous species, as shown in **Figure 1** [3], and one has to be very choosy in selecting this value. Most of these sensors operate at above room temperature range extending up to

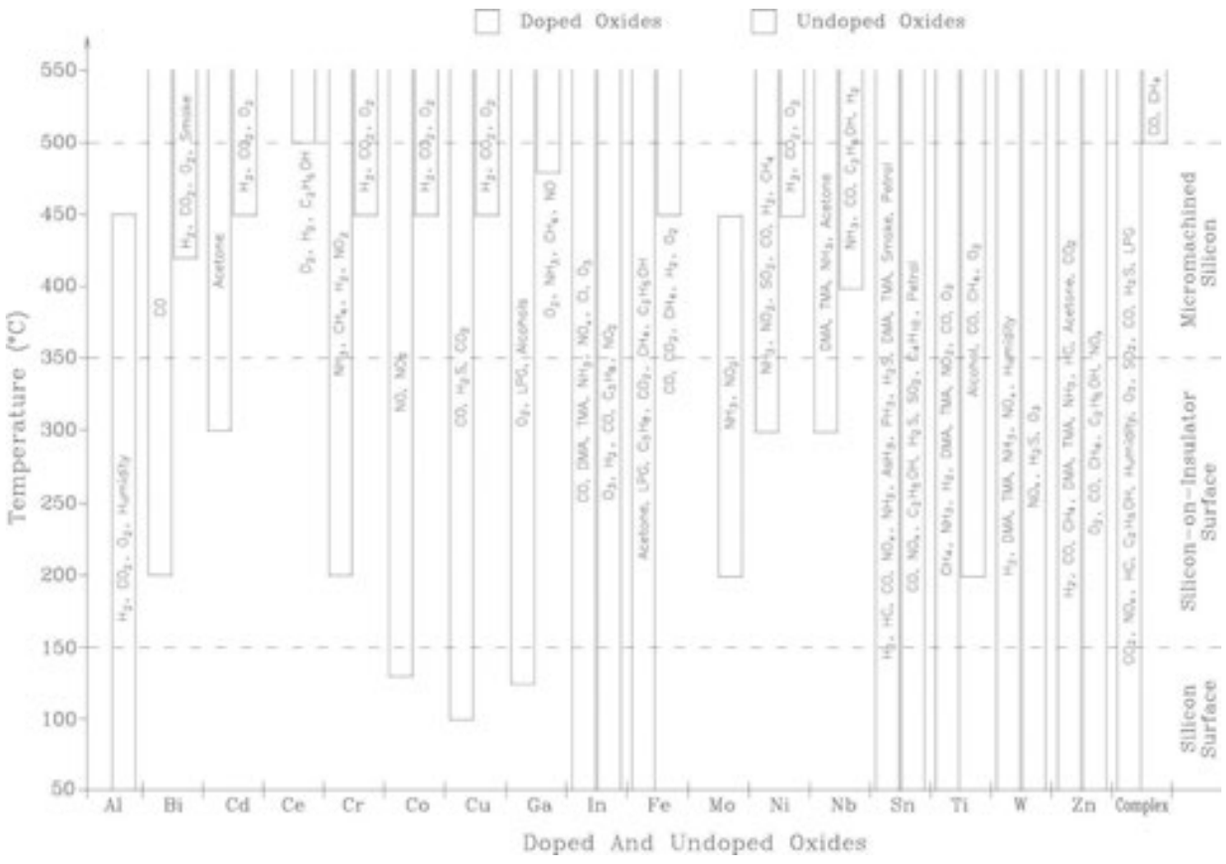

Figure 1. Gas sensing properties of different doped and undoped metal oxides for various gaseous species between the temperatures 50 and 500°C. The regions are placed adjacent to each other. Gaseous species are earmarked to each category. There are three different temperature zones that are identified here to create the required temperatures for the operation of the metal oxide-based sensor devices: on simple oxidized silicon wafer substrate (for operation from 50 to 150°C), SOI wafer surfaces (for operation from 50 to 350°C), and micromachined silicon MEMS structures (for operation from 50 to 500°C). For hybrid microcircuits using alumina substrates, the operating temperature ranges from 50 to 500°C and above ranges [3].

http://dx.doi.org/10.5772/62647

several hundred degrees centigrade, and it is necessary to know the correct operating temperature range of them. These values vary depending on the material and the detecting gaseous species. **Figure 1** shows the gas sensing properties of different doped and undoped metal oxides for various gaseous species between the temperatures 50 and 500°C. To create such temperature, we need a platform where these temperature zones maintain the required operating temperature. Here, three zones are identified for this purpose: simple silicon surfaces (from 50 to 150°C), silicon-on-insulator (SOI) surfaces (from 50 to 350°C), and micromachined silicon structures (up to 500°C). The other option is for hybrid microcircuits, where the operating temperature ranges from 50 to 500°C and above ranges. To obtain good sensitivity, one should know and operate these elements, accordingly.

First, molecular adsorption and desorption are mainly temperature-activated processes and thus decide many dynamic properties of the sensors, such as sensor response time and recovery times, and these parameters depend exponentially on this operating temperature. Surface coverage of the adsorbed species, co-adsorption, chemical decomposition or other reaction issues is also temperature dependent, resulting in different static characteristics of sensors that takes place at different temperature ranges. On the other hand, temperature has an effect on the physical properties of the sensor material, such as charge-carrier concentration, Debye length and work function. In most of the cases, the sensor sensitivity varies with the temperature. Initially, it increases gradually with increase in temperature and becomes less gradual subsequently at higher temperature ranges. With increase in temperature, it exhibits linear dependency initially but later ranges it deviates to non-linearity. This way it attains a maximum sensitivity value, and beyond this point of operation, the sensitivity falls rapidly showing a negative dependency with temperature. This type of behavior is being exhibited by almost all the metal oxide-based gas sensing materials. This is one possible reason for the decreasing sensitivity at higher operating temperatures. Some examples and their response behavior are shown below for most popular metal oxides.

Figure 2 shows the sensitivity graph illustrating the response of SnO_2 sensor to 100 ppm methane gas in dry air as a function of sensor operating temperature [1, 4]. Here, the sensitivity increases continuously from 300 up to 450°C, and this is the best performance point. If one exceeds this operating range, at higher temperatures, there is a negative influence to the sensitivity and it will fall. Subsequently, the sensor sensitivity with temperature changes from positive coefficient to negative coefficient values and degrades the sensor performance. Further, rise in temperature will reduce the sensitivity values considerably as shown in the figure. From the experimental results, one can identify and choose the best operating temperature range for the sensing element by carefully operating the sensor performance with temperature. In this combination, 425–475°C is the best operating zone. It is rare to get such symmetrical behavior of sensitivity values. The slopes and best operating temperature range are identified for this combination. No significant sensing property is possible beyond a specific temperature range, and the values are not good for signal analysis.

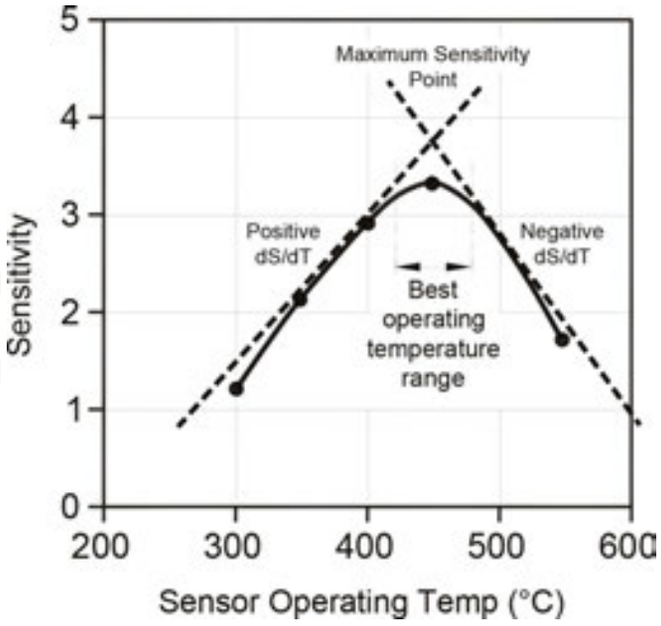

Figure 2. Response of tin oxide-based sensor to 100 ppm of CH_4 in dry air [1, 4] as a function of sensor operating temperature (in °C). Here, the sensor sensitivity, with operating temperature, changes from positive to negative values. Best operating temperature zone for the sensor combination is indicated. No sensing property is possible beyond a particular temperature range, and the recorded values are not good for signal analysis.

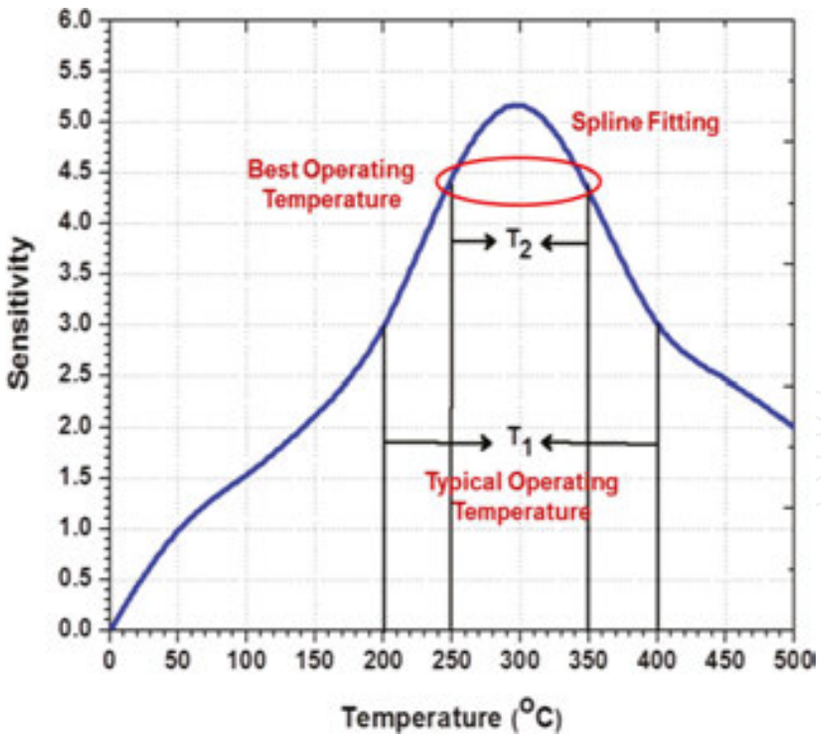

Figure 3. Typical zinc oxide sensitivity vs. temperature range for detecting 200 ppm CO gaseous species [5]. Both operating temperatures and best operating regions are identified for the data recorded using spline fitting. Beyond these ranges, the sensitivity becomes rather poor.

http://dx.doi.org/10.5772/62647

In the **Figure 3**, typical zinc oxide sensitivity with temperature is shown for the detection of 200 ppm carbon monoxide using zinc oxide sensing layer [5]. Both typical operating and best operating temperature regions are identified for the data recorded using spline fitting for the experimental points. Beyond these ranges, the sensitivity becomes rather poor. This material does exhibit sensitivity at lower temperatures, but the curve is not very symmetric in nature. The best operating temperature in this combination is seen to be between 250 and 350°C.

Similar characteristics are seen for the sensors using indium oxide material-based sensor for detecting 2 ppm of nitrogen dioxide gas, as shown in **Figure 4** [1, 4]. This is an important industrial raw material used in the synthesis of nitric acid. In this experimental observation, the sensitivity initially rises with temperature, and after reaching to a maximum value, it falls steadily moving towards a saturation stage after crossing the maximum sensitivity point. Here again, the sensor sensitivity with temperature changes from positive value to negative value. Best operating range is indicated here for sensor operation and is very narrow in these experimental results and is recorded between 165 and 185°C only. Positive slope indicates the reaction limited case, whereas the negative slope is due to binding energy of the gaseous species. At higher temperatures, the gaseous species fail to react with the sensor surface regions and are not detected.

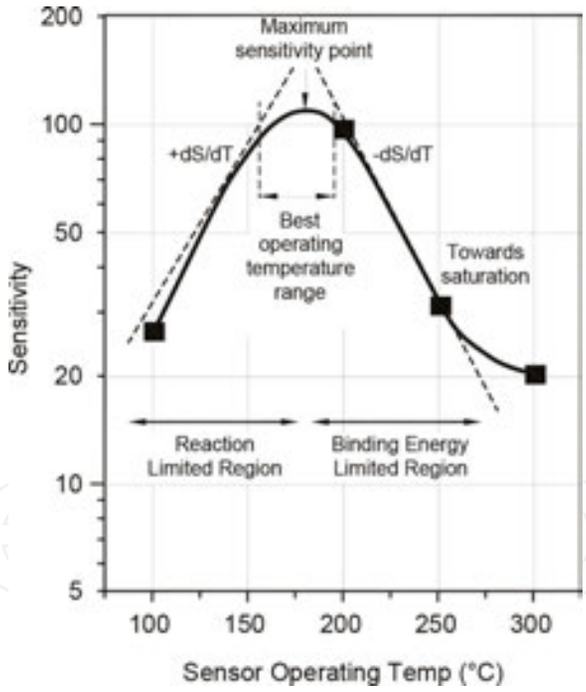

Figure 4. Response of indium oxide sensor to 2 ppm of NO_2 gaseous species as a function of sensor operating temperature (in °C) [1, 4]. Sensor sensitivity changes with the increase in operating temperature from positive value to negative values. Best operating range is indicated here for sensor operation to obtain useful signal for analysis. Positive slope signifies the reaction limited case, whereas the negative slope is due to binding energy of the gaseous species and fail to react with sensor surface regions.

Tungsten oxide also shows similar behavior as indicated in **Figure 5**. Here, the material sensitivity to 1 ppm nitrogen dioxide as a function of operating temperature is shown with

spline interpolation of recorded data [6]. Temperature in the range of 135–165°C is the best suited for this combination of gaseous species and sensing material. This is also relatively narrow region. According to Ghimbeu [6], the detection mechanism of nitrogen dioxide has some similarities to that of zinc oxide. It is considered that at low operating temperatures, these gas molecules are adsorbed on the WO_3 surface and forms nitrite type absorbents (ONO^-) and dissociates into nitrosyl-type absorbents (NO^-, NO^+). Hence, the response is related to the catalytic reaction of WO_3 with adsorbed species. The release of electrons from the surface increases the film sensitivity. The maximum sensitivity point here is 150°C.

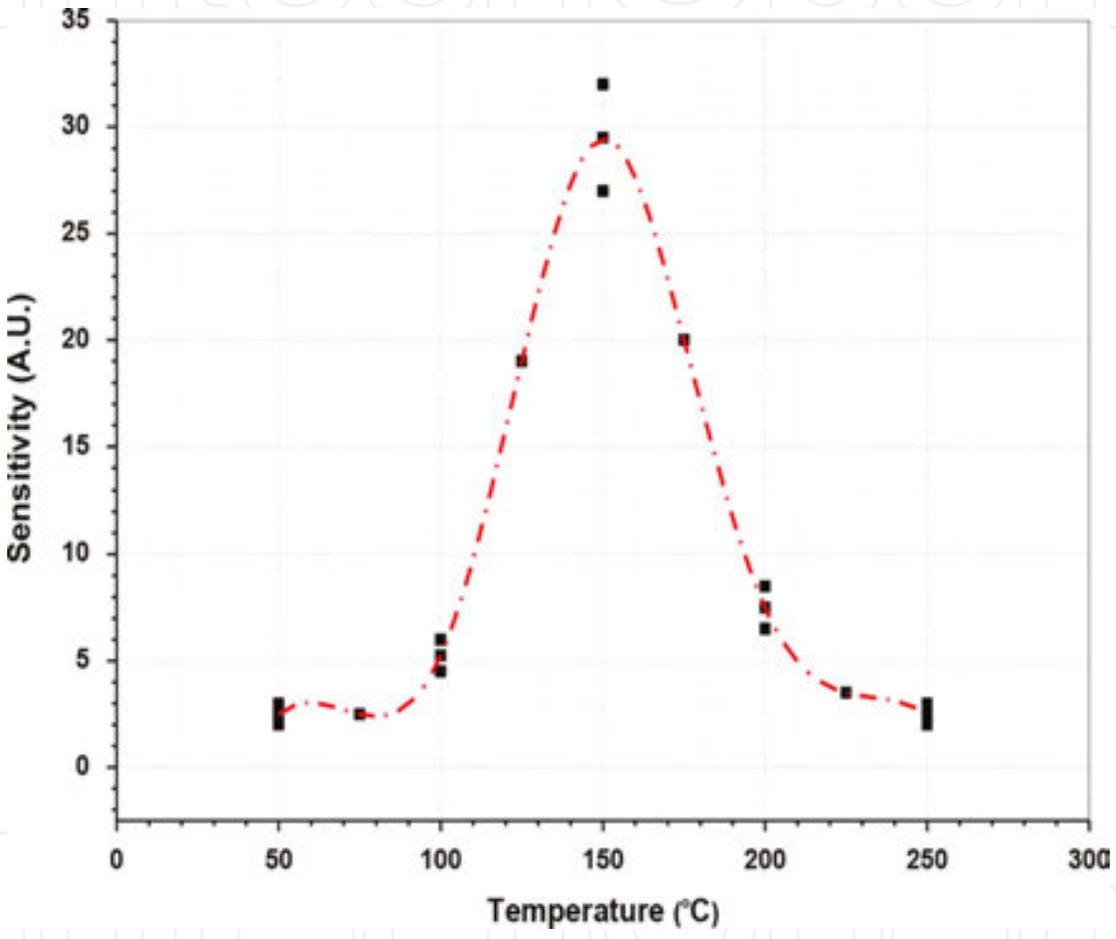

Figure 5. Tungsten oxide sensitivity to 1 ppm NO_2 as a function of operating temperature with spline interpolation of data. Data points are taken from Ref. [6]. Temperature in the range of 135–165°C is the best suited for this combination of gaseous species and sensing material.

4. Microelectromechanical structures (MEMS)

Silicon is the material used to create most of the integrated circuits used in the consumer electronics, and it has a major role in MEMS applications also. For many sensor applications, single-crystal silicon wafer, based on its intrinsic mechanical stability and the feasibility of

http://dx.doi.org/10.5772/62647

integrating sensing and the signal processing electronics on the same substrate, often presents an excellent substrate choice. This is a major point when compared with other substrate materials, such as glass, alumina, and hard polymers. For chemical sensors, the substrate is merely a working platform and its choice is not always straightforward. The silicon material has the highest cost per unit area, but this can be ignored by the small feature size possible in implementing silicon-based platforms. The silicon with its extreme surface flatness and well-established coating procedures often is the preferred substrate, especially for thin film-based sensing elements. The application of silicon device processing techniques to these miniaturized gas sensors results in low heating power, due to inherent low specific heat of silicon as a material, and a smaller spread in the electrical characteristics of silicon devices because of material uniformity in growing the silicon wafers. Owing to the low heat capacity of silicon material, this requires a heating power of the order of few milliwatts per any standard device. Reduction of power consumption is also a key aspect to reduce local thermal stress and also to obtain battery-operated devices for smart sensor applications including the field studies and to use in remote and inaccessible locations. These specific advantages have made silicon rather a convenient substrate for housing different gas sensing materials and to create high temperature zones required for sensing elements.

MEMS structures in silicon are fabricated either by bulk micromachining or by surface micromachining techniques. In the former case, the silicon substrate is etched by either wet chemical solutions or by vapor phase etching. Both anisotropic and isotropic etchants are used for this application. These etching steps are generally deeper and could etch out the silicon wafer depth to a level of 80–90% of the total thickness. The purposes of etchings aim to isolate the part, where high temperatures are to be created. Without these steps, it is difficult to stop the heat flow generated through the heating element mainly because of the good thermal conductivity of silicon and the generated heat spreads very fast into the bulk silicon. The thin platforms thus formed are used for placing the sensing element along with the heating elements. Etching to the predetermined depths in silicon wafer and the screening materials during the silicon for selective etching is very crucial and a challenging task.

In case of surface micromachining, an air gap is created using sacrificial layers. This created air gap prevents the heat flow to the bulk silicon and reduces the body thermal mass. The sacrificial oxides are typically deposited through low temperature CVD process and are etched out at a later stage to create the physical gaps. Many options are available for this purpose to create/deposit the sacrificial layers. Platform structures are selected such that they are thermally stable, mechanically stronger, and HF acid-resistant materials. These are mandatory as the material has to withstand high temperature operation and should not deform during their operation. At the time of etching of the sacrificial oxides, the platform material must show inertness to the etchant. In this category, only two material options are possible. They are LPCVD polycrystalline silicon and LPCVD silicon nitride films. In case of polycrystalline silicon films, it satisfies all the three requirements. HF-based solutions do attack silicon nitride, but the etch rates are very low in comparison with the sacrificial oxides. In this study, both options are used for platform formation and the experimental observations are reported.

Figure 6 shows the SEM image of platform release using sacrificial oxide lateral etching technique for the creation of air gap on silicon surface [7]. For this purpose, a blanket CVD oxide, to a desired thickness, was deposited at low temperature on a fresh silicon wafer. Anchor points are defined selectively using photolithography technique, and the oxide was removed from these portions. Polysilicon was subsequently deposited, and the platform area is defined with photolithography technique again. Unwanted polysilicon portions were etched out and also the CVD oxide underneath it. Platform release experiment was carried out by immersing the complete wafer and was examined periodically for the status sacrificial oxide. In this picture, the platform is not fully released. Since the film is transparent, at this thickness value, the sacrificial oxide is clearly visible through the platform body. The sacrificial oxide regions are totally removed under the supporting arms because of low lateral distances, and the freed supporting structures of platform are visible clearly in the figure. **Figure 7** shows the closer view of the measurements of the created air gap highlighting one of the corner portions of the platform [7]. The vertical measurements were done to confirm the air gaps created in this approach. The slight variation depends on the sacrificial oxide thickness uniformity and also due to errors in marking the regions. Tilt of SEM image capture has its limitations and direct air gap measurements are rather difficult.

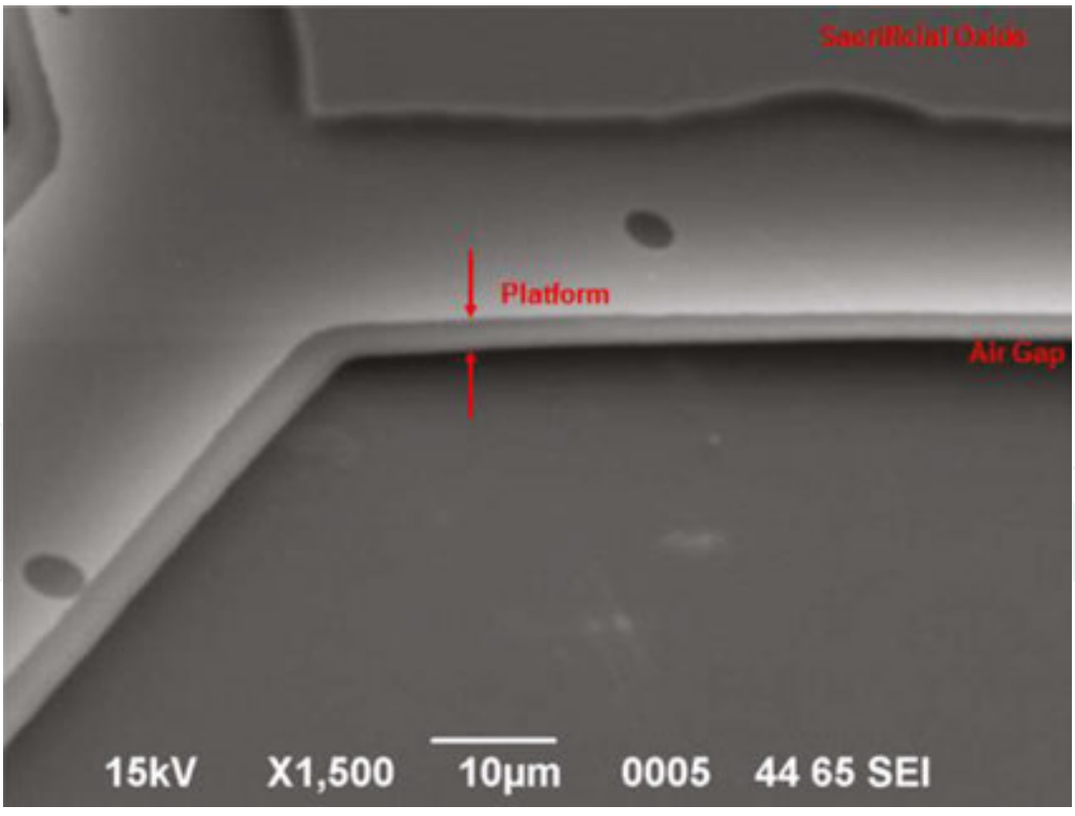

Figure 6. SEM image of platform release using sacrificial oxide lateral etching technique for the creation of air gap on silicon surface [7]. Here, the platform is not fully released. The film is transparent, at this thickness value, and the sacrificial oxide is clearly visible through the platform body, whereas the sacrificial oxide regions are totally removed under the supporting arms because of low lateral distances.

http://dx.doi.org/10.5772/62647

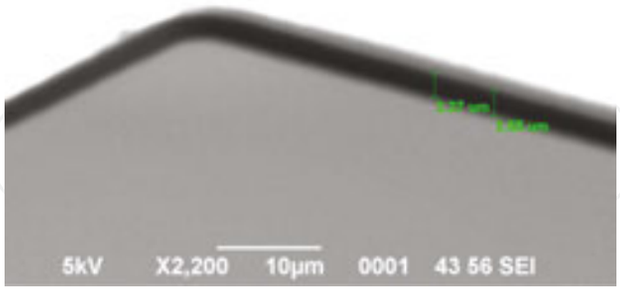

Figure 7. SEM image of platform released by surface micromachining structure on silicon surface highlighting one of the corner portions [7]. The vertical measurements were done to confirm the air gaps created in this approach.

Figure 8 shows the different popular platform structures used for this application. In this test structure, all these shapes are defined and were subsequently etched for releasing the platforms. This figure shows the lateral etching of sacrificial oxide and the platform status of release. The etch front and the released corners are shown in this SEM images. **Figure 9** shows the similar experiment with LPCVD silicon nitride using lesser sacrificial oxide thickness, that is 1.0 μm. These silicon nitride films were densified to reduce the HF acid effect during the platform release. This optical photograph shows the fully released thin film silicon nitride structures.

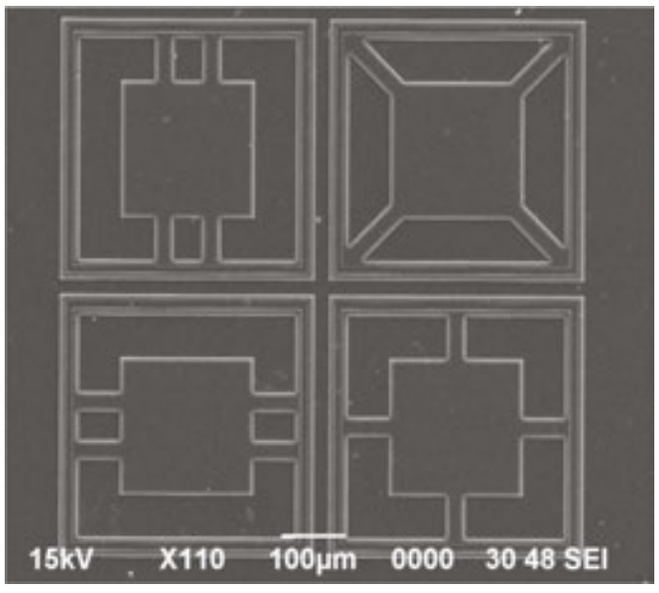

Figure 8. Polycrystalline silicon platform suspension structures for creating an air gap of approximately 3.0 μm [7]. This polysilicon was deposited by LPCVD technique based in silane chemistry. These platforms are in the process of release using surface micromachining technique. Figure shows the lateral etching of sacrificial oxide, and the platforms are semi-transparent at this thickness. The etch front and the released corners are shown in this SEM images.

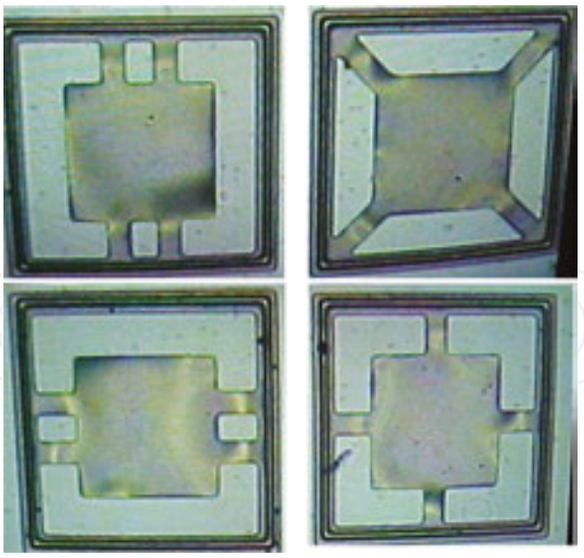

Figure 9. Optical micrographs of different suspended and released silicon nitride platforms by surface micromachining technique on silicon substrates [7]. These nitride films were deposited using LPCVD technique using dichlorosilane- and ammonia-based chemistry. Films were subsequently densified prior to releasing the platform structures. Sacrificial oxide portions are completely removed using hydrofluoric acid-based solutions.

A test run for these release experiments provides enough information to estimate the time durations to complete the entire process. As these structures will reduce the thermal mass considerably and greatly reduces the power dissipation to raise the platform temperatures. They also respond very fast to the changing measurement conditions and exhibit quick thermal response in maintaining the temperatures. The lateral etching and removal of the complete sacrificial layer are time-consuming processes, and the process bound wafer experiences other technology-related issues because of long time contact of hydrofluoric acid. To avoid such time delay, perforated platforms are proposed and many scientific teams are working in this issue. This method reduces the time, but the advantage of perforation limits the mechanical strength of the platform and disturbs the temperature distribution on it. However, there are several practical difficulties in realizing the complete gas sensor devices on these released platforms. Releasing these thin diaphragm platform is a serious technology issue and often decides the yield.

5. Air-suspended structures

To avoid technological limitations, as discussed above, an attempt is made to use the silicon wafer directly as a platform for the required temperature distribution. When compared with the thickness of MEMS platform, say few microns, the bulk silicon wafer thickness is much larger and consumes proportionately larger power. However, the mechanical strength and temperature distributions advantages are not negligible and the device can be put to use for gas sensing applications. As discussed earlier, most of the metal oxide sensors work at higher temperatures, of the order of few hundreds of centigrade, heating the complete silicon die is worth to note. No mechanical issues are reported for silicon in this temperature range and are

http://dx.doi.org/10.5772/62647

stable to operate for longer periods. It is also important to note the temperature of the platform to monitor and also to control it to the desired ranges.

In most of the cases, the heating element is made up using platinum metal. This material has been widely used for harsh environment and also known for its standard in many industrial applications. It is chemically inert, and no electrical parameter drifts are reported. In this case, we have used this material and the same is sputter deposited on to the substrate for this application. Standard photolithography and lift-off technique is used for defining the heater for this purpose. Substrates were properly cleaned before the deposition step was carried out. Adhesion layer is used to enhance the adhesion of the film. Defining both the heater and platinum resistance thermometer (PRT) together has certain operational advantages. However, getting a standard PRT is a difficult task and one can define the platinum resistor along with the heater and calibrate it to the desired temperature range is a better option to know the exact temperature value.

Figure 10. Testing of platinum micro-heater (4 × 5-mm size) on 1-mm-thick alumina substrate up to red hot temperature ranges.

To verify the micro-heater performance, platinum metal was deposited on 1-mm-thick polished alumina substrate and was defined by lift-off technique [8]. Each heater die was measured as 4-mm × 5-mm, and the electrical contacts were made to the heater pads to check the performance. DC current was applied, in steps, to know the heating of the alumina substrate. For temperature measurement purpose, a thermocouple was placed on the back side

of the alumina heater to measure the exact temperature directly. Heater current was increased further till the red hot condition was observed on the alumina substrate. **Figure 10** shows the testing of this micro-heater up to red hot temperature ranges. Through this experiment, we gained confidence to operate these heaters to a value not exceeding 500°C, the required temperature for most of the metal oxide-based gas sensing devices.

Figure 11 shows the PRT resistance variation with the measured temperature using a thermocouple attached to the backside of the alumina substrate. The alumina die size is same in this case also. Both the heater and PRT are defined on the same side of the polished alumina substrate, and the electrical contacts were made to them to measure the current rating. Platinum thickness is arbitrarily selected for this study, and we avoided the theoretical prediction of the PRT resistance values. Only DC current, through a constant current supply source, is applied for the heater pads to raise the platform temperature. Variation of PRT resistance and the temperature measured was recorded. The experiment was repeated at different values of heater current (in mA). Both the values are recorded to study the behavior. These experimental observations corroborate the functionality of both heater and defined PRT on the alumina substrate.

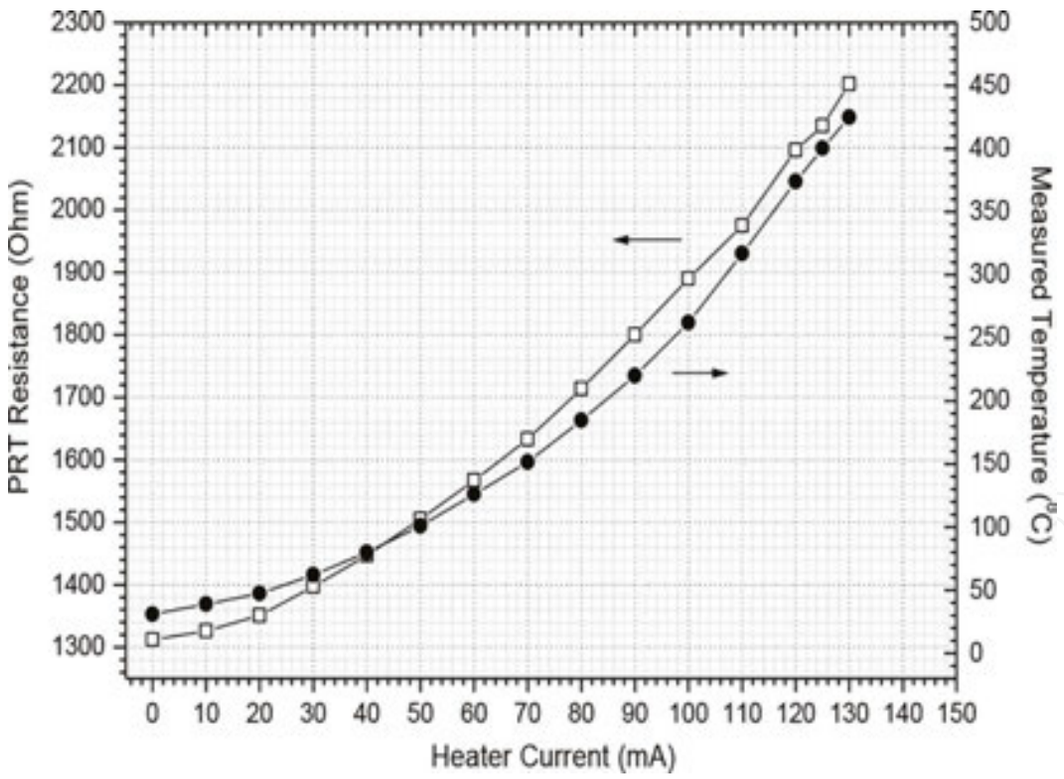

Figure 11. PRT resistance variation with measured temperature using thermocouple attached to the backside of alumina substrate. Data are drawn together to the same experimental points. Measured temperature is recorded through the thermocouple attachment and using standard calibrated system which converts the thermocouple emf values to equivalent temperature. In this case, the alumina substrate is one-mm thick and the die size is 5 × 4-mm defined area. Heater and PRT are defined on the same side of the substrate. Pt thickness is arbitrarily selected for this study, and DC current is applied for the heater pads.

http://dx.doi.org/10.5772/62647

Air-suspended structures suffer from thermal equilibrium issue even though they are defined on the same side on alumina substrate. Heating in these structures draws more power because of larger mass when compared with the thin MEMS platform structures. The thermal equilibrium may take couple of minutes to reach the equilibrium stage. Hence, this thermal response time issue will remain with these structures and that influences the sensor response and recovery time values.

6. Fabrication of sensing element, PRT, and heater structures

The electrical conductivity is a critical issue for the sensing element and systematic measurement of it is very important to the functionality of sensor. The resistance of thin film consists of three parts: (i) bulk resistance, (ii) surface resistance, and (iii) contact resistance between metal electrodes and the oxide-semiconducting films. However, for practical applications, all these three values are considered as a single entity and the total resistance is directly accepted as the sensing element resistance.

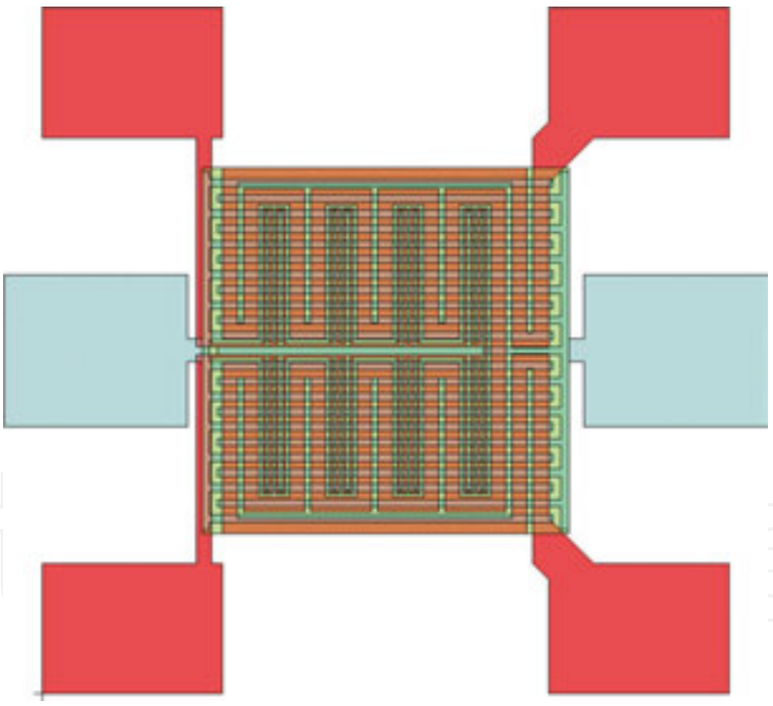

Figure 12. Design for heater and PRT configuration to raise the sensing layer temperature [7]. Both heater and PRT are defined by single photolithography step, and the total area is covered by the sensing film as shown above. Interdigitated structure measures the changes in electrical resistance of the sensing layer. Here, all the layers are electrically isolated with CVD oxides where applicable.

For air-suspended silicon micro-bridge structures, we have designed a structure such that both the PRT and heater components are defined in a single photolithographic step. After the definition of this PRT embedded heater, the total area is covered with a sensing layer to be

used for gas sensing applications. This sensing layer will be directly interacting with the atmosphere, where surface reactions take place. To measure the sensing layer conductivity variations, an interdigitated structure is defined and placed directly on this layer. The ideal metal is gold and is preferred because of its inertness in the atmosphere conditions. Electrical isolation is done with low temperature-deposited CVD oxides to bury the heater and PRT structures. Contact windows are opened on the pad areas for wire bonding. **Figure 12** shows the complete design, where PRT, heater, sensing element, and interdigitated structures are designed. For clarity, the CVD isolation oxides are not shown in this figure.

For the deposition of platinum and also for the sensing layer, reactive RF sputtering method is used. The depositions are carried out in an oil-free ultra-high vacuum chamber using suitable target materials as per the thickness requirement. Sputtering is done in the argon plasma environment, and the vacuum conditions are closely monitored. Depending on the requirement of film thickness, a predetermined time and RF power values are estimated and the depositions are carried out accordingly. Sometimes film thickness monitors are used to monitor the growing films. **Figure 13** shows the RF sputtering process inside the high vacuum chamber. **Figure 14** shows the photograph of platinum thin film deposited on oxidized 3-inch-silicon wafer using this technique.

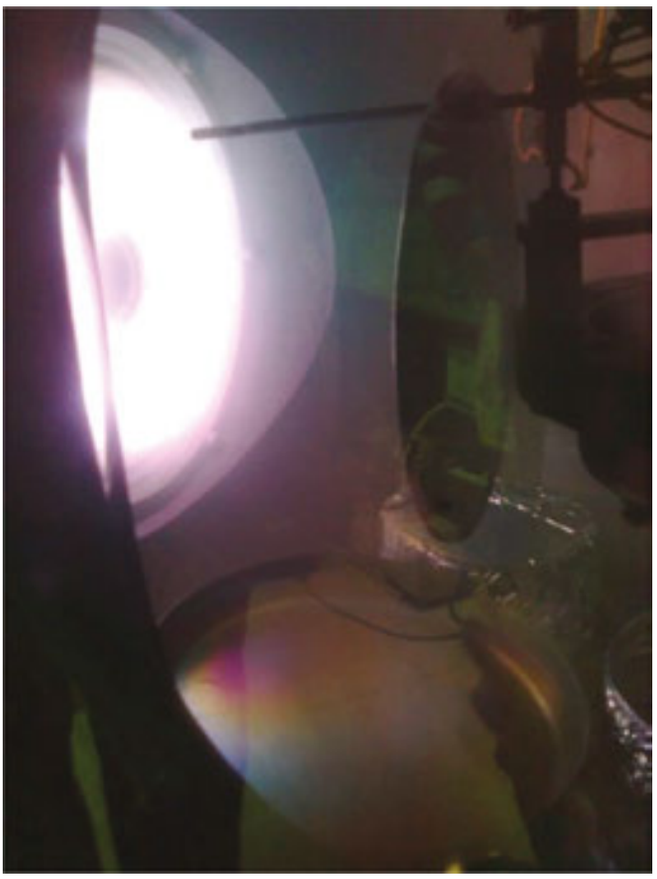

Figure 13. Typical RF sputtering process inside the vacuum chamber, under ultra-high vacuum conditions, to deposit platinum metal used for defining PRT and heater configurations.

http://dx.doi.org/10.5772/62647

Figure 14. Photograph of platinum thin film deposited on oxidized three-inch-silicon wafer by RF sputtering technique.

Figure 15 shows the photograph of PRT embedded micro-heater configuration defined on silicon. This structure is realized using photolithography combined with lift-off technique [8]. The left side of the picture pads shows the PRT connection, whereas the right hand side is meant for the heater configuration. Using this base structure, many sensors can be realized on this. Because of line width difference, the resistance values of PRT and heater vary very widely. Optimization is necessary for the thickness of the platinum film to get calibrated values. To simplify the PRT, a new design was realized to reduce the resistance values very close to the practical values. **Figure 16** shows the simplified version of PRT embedded micro-heater, for a purpose built structure of 5-mm × 4-mm, to create low to moderate temperatures on silicon surfaces particularly suitable for metal oxide-based gas sensing materials [9]. **Figure 17** shows the fabricated devices at wafer level.

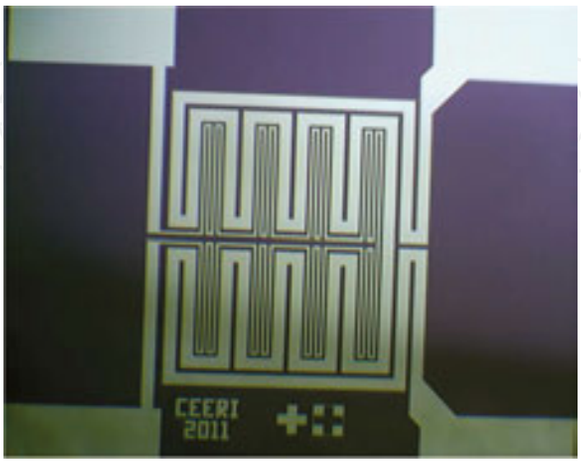

Figure 15. Photograph of PRT embedded micro-heater configuration on silicon. The structure is realized by photolithography and lift-off technique.

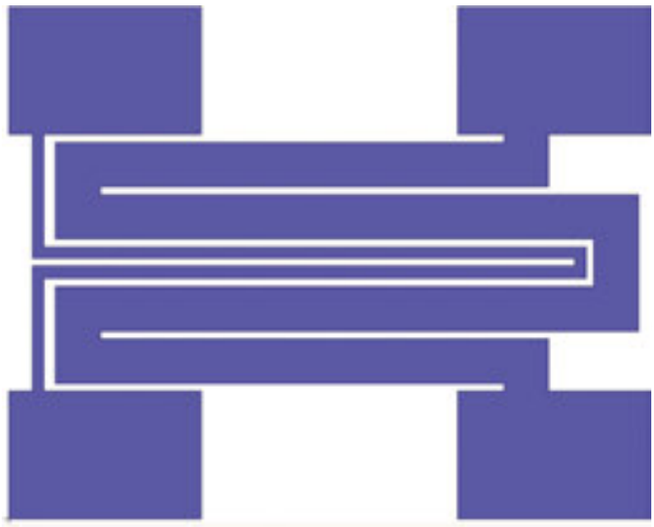

Figure 16. Simplified version of PRT embedded micro-heater, for a purpose built structure of 5 × 4-mm, to create low to moderate temperatures on silicon surfaces suitable for metal oxide-based gas sensing materials [9].

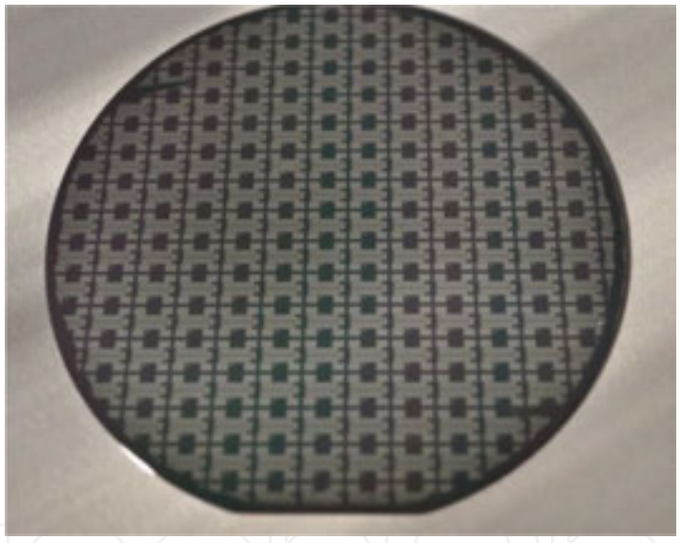

Figure 17. Realization of PRT embedded micro-heater on a 3-inch oxidized silicon wafer [7, 9] using platinum RF sputtering and lift-off methods.

Subsequently, all the dies are separated by standard dicing method and wire bonding was carried out on the defined pad areas. These bonded platforms are connected to a structure to verify the temperature distribution of the micro-heater on these air-suspended micro-bridge structures [9] as shown in **Figure 18**. In this structure, the air acts as a barrier and the heat generated by the heating element initially distributes within the bulk of silicon by thermal conduction process. The heat that escaped through the contact pads is much less when compared to the air convection. This air convection has a greater role in the heat loss mechanism. A closed package housing encloser with proper opening is a possible solution for these proposed structures to avoid convection-related issues.

http://dx.doi.org/10.5772/62647

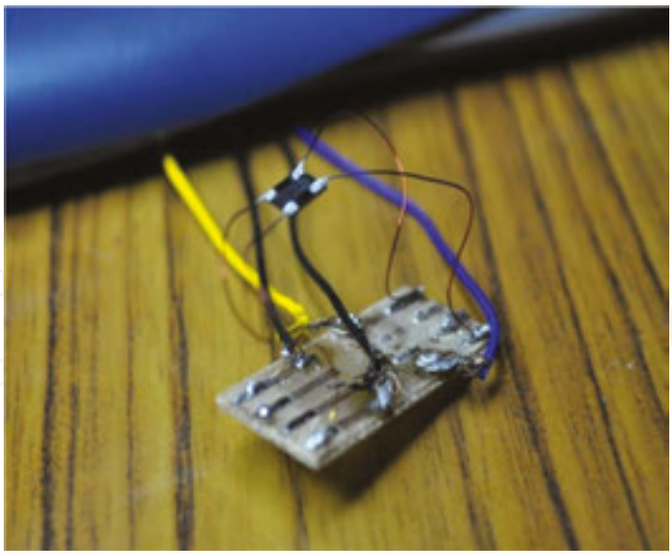

Figure 18. Wire bonding to verify temperature distribution of the micro-heater on air-suspended silicon micro-bridge structures [9].

Resistance calibration of the platinum PRT is necessary to operate the heater more accurately. It is the PRT value that controls the heater current, and the true values are relevant here. **Figure 19** shows the calibration of PRT (top) and micro-heater (bottom) using standard temperature bath up to 500°C to the structure as per the design shown in **Figure 16**. Here, both the values are stable and are repeatable within the shown range. Figure also shows that the heater will heat up the platform and automatically raises the PRT resistance value signifying the temperature raise. This raises the sensing layer temperature to the required level for the sensor operation.

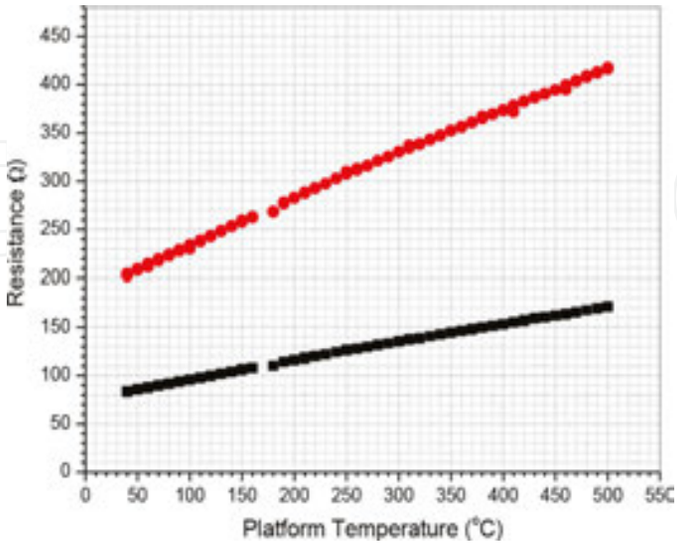

Figure 19. Resistance calibration of the platinum PRT (top) and micro-heater (bottom) using standard temperature bath up to 500°C to the structure as per the design shown in **Figure 16**.

7. Reliability of bulk micro-bridge structures

In most of the cases, the heating element is made up using platinum but polysilicon and nichrome heaters are also reported for this purpose. Not many encouraging publications are found in case of the later materials. Some experiments were carried out with the structure as shown in **Figure 15** in an open environment with minimum air turbulence. **Figure 20** shows the PRT incremental resistance with 1 mA DC constant and continuous heater current with the silicon substrates. Only at the initial stages, there is a rise but within 15 min, the complete die reaches to thermal equilibrium. It is expected that in a closed environment, this time delay may be brought down to couple of minutes. Heating element is placed on one side of the substrate surface and generated heat is slowly distributed into the bulk silicon. This is a time-consuming process.

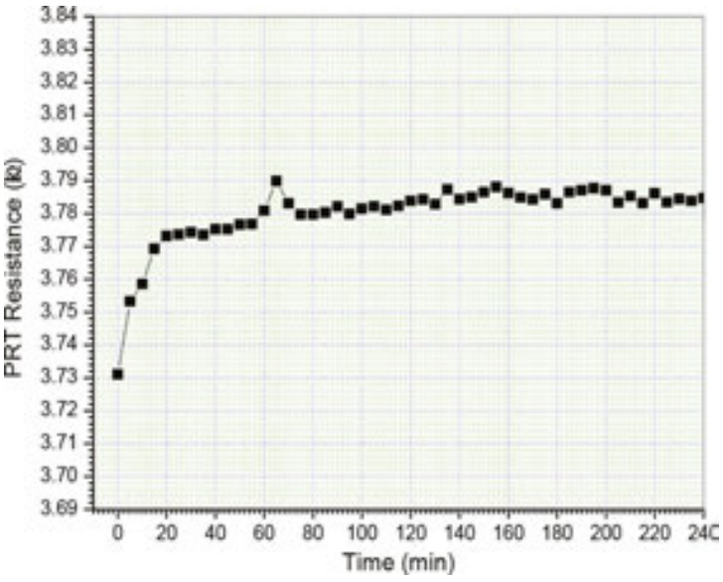

Figure 20. PRT incremental resistance with 1 mA DC constant and continuous heater current with silicon substrates to the structure as shown in **Figure 15** [7].

Thermal hysteresis has been found in these structures because of silicon wafer thickness. **Figure 21** shows the thermal hysteresis measurement of PRT and the heater on oxidized silicon substrate to the design structure shown in **Figure 15**. The circles are during increasing DC current steps, and square points are while decreasing cycle. Here, the current is passed through the micro-heater pad connections. In these recordings, 5 min time gap (delay time) was maintained between apply the heater current and measure the PRT resistance values [7]. The delay is mainly aimed for temperature rise and better uniformity in the bulk of silicon substrate. Despite the delay, a clear thermal hysteresis is seen at 1 mA current setting.

The stability of both PRT and heater was carried out over a period of time, and **Figure 22** shows the results for the structure shown in **Figure 15**. The bottom points correspond to the heater and the top ones to the PRT. These air-suspended silicon micro-bridge structures were carried out in the temperature range between room temperature and 500°C. The structure is very stable

http://dx.doi.org/10.5772/62647

for long-time operations up to 400°C, but beyond this range, both PRT and heater values become unstable as shown in the figure. The observed values scatter very randomly. Between 450 and 500°C, the structure becomes mechanically unstable, and ultimately, it fails to provide reliable values. Hence, the entire system is safe to operate up to a value of 400°C. This temperature is sufficient for many sensing materials and cover good number of sensing materials.

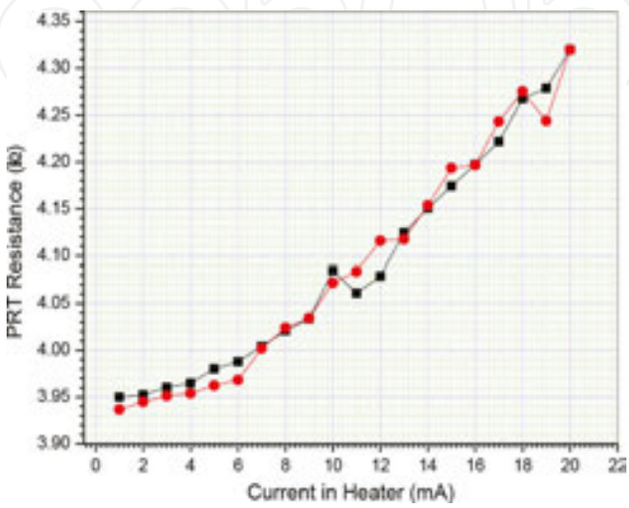

Figure 21. Thermal hysteresis measurement of PRT and heater on oxidized Si substrate to the structure shown in **Figure 15**. The circles are during increasing steps and square while decreasing the current passed through the micro-heater. Here, 5 min time gap was maintained between apply the current and measure PRT resistance values [7]. The delay is mainly aimed for temperature rise and better uniformity in the bulk of Si substrate.

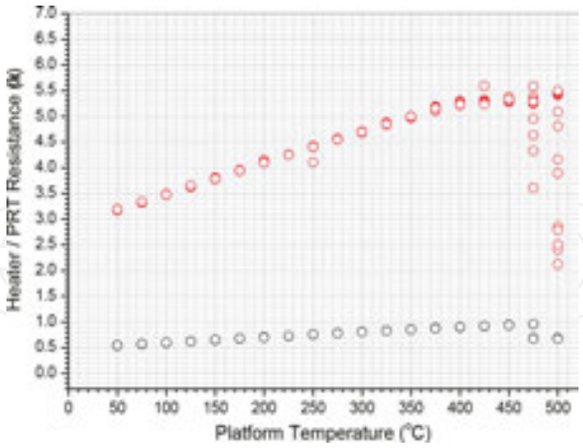

Figure 22. Response of air-suspended silicon micro-bridge structures in the temperature range between room temperature and 500°C. The structure is very stable for long time operations up to 400°C, but beyond this range, both PRT and heater values become unstable as shown. Between 450 and 500°C, the structure becomes mechanically unstable and ultimately it fails.

The structure of heater and PRT configurations can be simulated using ANSYS® software for any specific configurations to achieve the required temperature distribution as per the

requirement of sensing film and its physical shape. Necessary physical parameters are to be provided for the realistic simulation. The final temperature distribution, for a specific configuration, as indicated in **Figure 16** is shown in **Figure 23**. Here, the temperature distribution of the micro-heater temperature, operated at 5 V DC applied voltage, is shown. From the results, it is very clear that the center of the suspended platform will have the maximum temperature value. In these locations, the sensing layer needs to be distributed accordingly to enable the element experiences the required temperature for better performance. This way one can select the required temperature and approach the desired properties by applying suitable voltages. This is easy for most of the field applications and to achieve the desired temperature ranges to use the metal oxide-based sensing layers for sensing applications. At this temperature, there are a wide variety of material combinations [9] one can select to detect different gaseous and VOC species. By simulation of temperature and its distribution, it is possible to realize the devices based on air-suspended micro-structures for gas sensing applications.

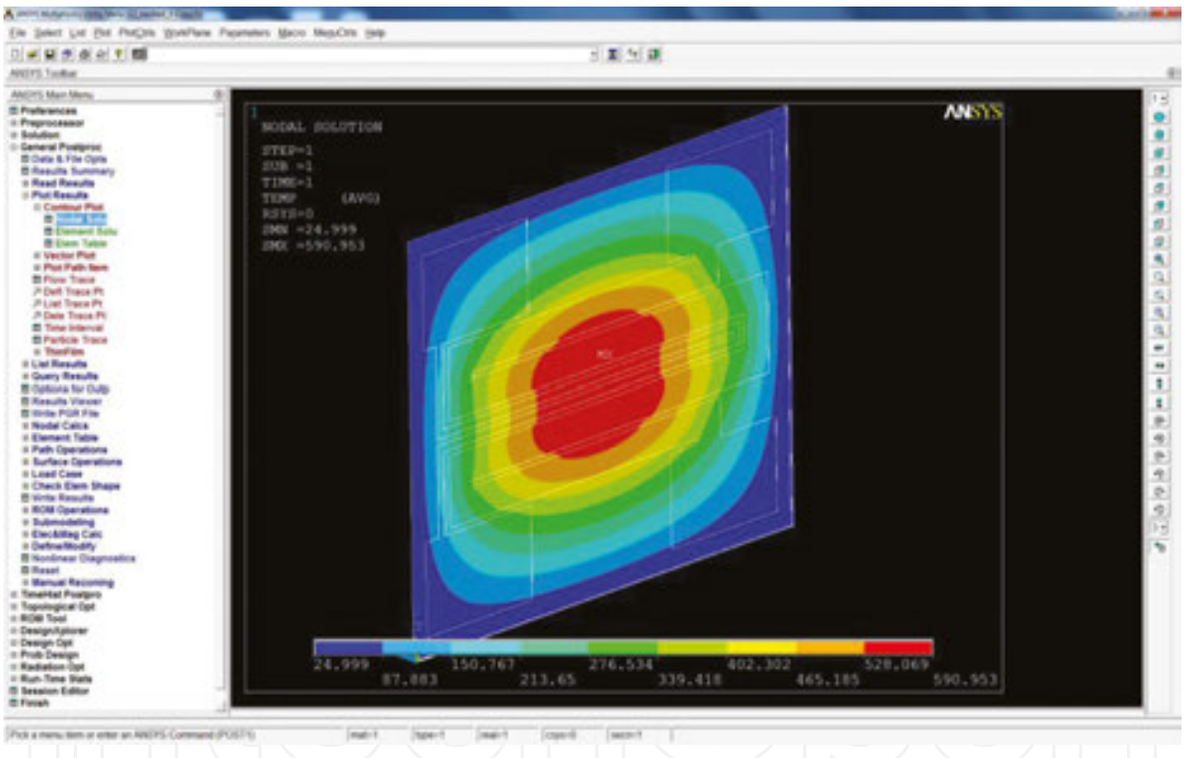

Figure 23. Typical nodal temperature contour plot with 5 V DC input for the structure, as shown in **Figure 16** using battery-operated device. Image is generated by simulation using ANSYS® by providing realistic parameters values [9].

Placing the structures in a sealed environment with a metal mesh opening is a better option to operate these devices. Standard microelectronic packaging is not useful at the heater temperatures. Useful device packages for these micro-bridge gas sensors are proposed in this study. The package structure, as shown in **Figure 24**, which is a standard package used for Toshan LPG gas detector sensor MQ6 [10], appears to be useful. Interaction of atmospheric gases takes place through this metal mesh and the air suspension provides the required thermal isolation from the heating element.

http://dx.doi.org/10.5772/62647

Figure 24. Useful device package structures for the air-suspended micro-bridge gas sensors proposed in this study. Shown here is a package used for Toshan LPG gas detector sensor MQ6 [10]. Courtesy: amazon.in. Source: internet.

8. Conclusions

In this chapter, we mainly focused for creating and maintaining specific temperature ranges useful for most of the gas sensing materials, particularly for metal oxide-based thin film layers, to operate them more efficiently to detect different gaseous species at different concentration levels. For practical devices and also for field applications, battery-operated micro-gas-sensors with air-suspended silicon bulk micro-bridge structures are discussed from the practical usage point of view. This avoids both the bulk and surface micromachined MEMS configurations. Power dissipation and the required temperature stability are discussed to operate the best operating temperature zones for getting a stable and reliable signal. Air-suspended structures are highlighted, and a comparison is drawn between simple and MEMS-based structures from the fabrication point of view. Ease of fabrication and operation limitations are also explained with structure reliability in usage.

Acknowledgements

The authors would like to thank DIT, Govt. of India, New Delhi (DeitY), for project sponsorship at CSIR-CEERI Pilani, India, where some of the experimental work was carried out, and for executing them for VOC gas sensor development for detecting pollutant gases using metal oxide-based thin film structures.

Author details

Keshavaditya Golla[1*] and Eranna Golla[2*]

*Address all correspondence to: keshav.aditya19@gmail.com and eranna.mems@ee.iitm.ac.in

1 Institute for Automation and Electrical Engineering, University of Applied Sciences Bremerhaven, Bremerhaven, Germany

2 Centre for NEMS and Nanophotonics, Department of Electrical Engineering, Indian Institute of Technology, Madras, India

References

[1] Eranna G., Metal Oxide Nanostructures as Gas Sensing Devices, CRC Press (A Taylor & Francis Book), New York, 2012, ISBN 978-1-4398-6340, and the references therein.

[2] Jonda S., Fleischer M. and Meixner H., "Temperature control of semiconductor metal-oxide gas sensors by means of fuzzy logic", *Sensors and Actuators*, B34, pp. 396–400, 1996.

[3] Eranna G., Joshi BC, Runthala DP and Gupta RP, "Oxide materials for development of integrated gas sensors—A comprehensive review", *Critical Reviews in Solid State and Materials Sciences*, 29, pp. 111–188, 2004, and the references therein.

[4] Niederberger M., Garnweitner G., Pinna N. and Neri G., "Non-aqueous routes to crystalline metal oxide nanoparticles: Formation mechanisms and applications", *Progress in Solid State Chemistry*, 33, pp. 59–70, 2005.

[5] Eranna G., Dwivedi M. and Vyas Vimal, "Optimization of ZnO thin film sensor for CO detection using MEMS structures", National Symposium on Materials for Advanced Technology (NSMAT-2011), March 27, Banasthali University, Banasthali, India, 2011.

[6] Ghimbeu CM, "Preparation and characterization of metal oxide semiconductor thin films for the detection of atmospheric pollutant gases", Thesis, Presented at the University Paul Verlaine of Metz, November 2007.

[7] Eranna G., Project on Development of MEMS based integrated micro gas sensor for VOCs and pollutant gases, Grant-in-Aid Project from Department of Information Technology (DeitY), Govt of India, New Delhi.

[8] Eranna G., Joshi BC, Bhargava J., Sharma AK, Kothari P. and Laxmi S., "A new lift-off technique to define fine platinum metal features using CVD sacrificial layers", Patent pending.

[9] Keshavaditya G., Eranna GR and Eranna G., "PRT embedded microheaters for optimum temperature distribution of air-suspended structures for gas sensing applications", *IEEE Sensors Journal*, 15 (7), pp. 4137–4140, 2015.

[10] https://www.google.co.in/webhp?sourceid=chrome-instant&ion=1&espv=2&ie=UTF-8#q=Toshan LPG gas detector sensor MQ6.

IntechOpen

IntechOpen